Synthesis and Oxidation of Silver Nano-particles

Hua Qi*, D. A. Alexson, O.J. Glembocki and S. M. Prokes*
Electronics Science and Technology Division,
Naval Research Laboratory, Washington, DC 20375
huaqi@ccs.nrl.navy.mil; sharka.prokes@nrl.navy.mil

ABSTRACT

We demonstrated a fast and easy way to synthesize Ag nanoparticles (NPs) on ZnO nanowires (NWs) and silicon substrates by an electroless (EL) plating approach. ZnO NWs used here were grown via vapor-solid (VS) mechanism at 560 ºC for 30 min. The stability to oxidation of these EL-produced homogeneous Ag NPs on ZnO nanowires was investigated by surface enhanced Raman spectroscopy (SERS), showing that the attachment of thiol to the Ag surface can slow down the oxidation process, and the SERS signal remains strong for more than ten days. Furthermore, we examined the surface oxidation kinetics of the Ag NPs as a function of NPs size and size distribution by monitoring the oxygen amount in the composites using energy dispersive x-ray (EDX). Results indicate that the EL plated Ag NPs show faster oxidation rates than those produced by e-beam (EB) evaporation in air. We attribute this to the fact that the EL produced silver particles are very small, in the 20 nm range, and thus have high surface energy, thus enhancing the oxidation. These studies provide extensive information related to the Ag NP oxidation rates, which can help in extending the Ag lifetime for various applications.

Keywords: silver nanoparticles (NPs), oxidation kinetics, electroless (EL) silver plating, surface enhanced Raman spectroscopy (SERS), energy dispersive x-ray (EDX)

1. INTRODUCTION

Nano-particles (NPs) have attracted much attention due to their potential applications in catalysis, biology, computing, solar cells and optoelectronic devices [1-5]. For example, silver (Ag) NPs have been widely used to enhance the surface sensitivity of some spectroscopic measurements, such as fluorescence, Raman scattering, and second harmonic generation. Researchers have reported many different ways to produce silver NPs, such as photochemistry, electrochemistry, chemical reduction, microwave processing, ultra-sound processing, gamma irradiation, ion irradiation, plasma processing, electron irradiation etc. [6-14], to meet the requirement of various applications. However, the oxidation process is seldom studied in detail on the nanoscale. Here, we employed an easy and reproducible electroless approach to synthesize silver NPs on ZnO NWs and on a bare silicon surface, and we have investigated the silver oxidation rates by monitoring surface enhanced Raman spectroscopy (SERS) signal and by energy dispersive x-ray (EDX) techniques. The results

Quantum Dots and Nanostructures: Synthesis, Characterization, and Modeling VIII,
edited by Kurt G. Eyink, Frank Szmulowicz, Diana L. Huffaker, Proc. of SPIE Vol. 7947,
79470Y · © 2011 SPIE · CCC code: 0277-786X/11/$18 · doi: 10.1117/12.871122

indicate that a self assembled monolayer of benzene thiol on the silver NPs can slow down the oxidation of silver to a certain extent. Further quantitative investigation demonstrated the size and size distribution of the silver NPs also play important roles in the oxidation rate.

2. EXPERIMENTAL DETAILES

2.1 Growth of ZnO NWs

ZnO nanowires were grown in a horizontal furnace under flowing Ar atmosphere at 560 ºC for 30 minutes. No catalyst was used and growth was performed on a Si (100) substrate [15]. In this process, Zn powder was placed at one end of a quartz boat, and the substrates were placed a set distance from the powder, as shown in scheme 1.

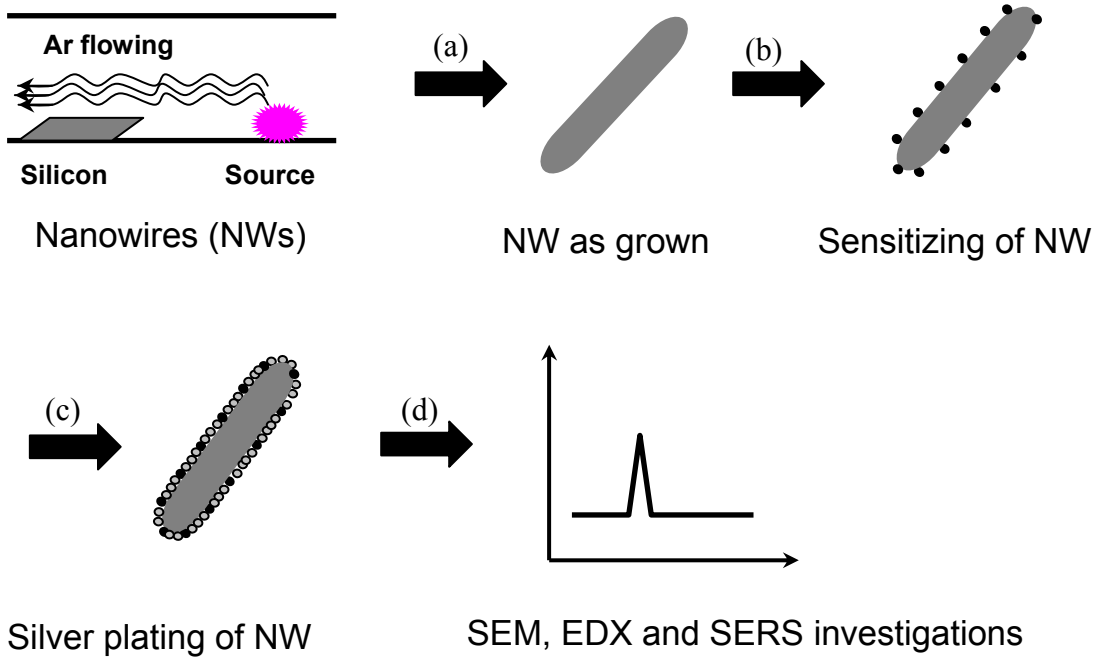

Scheme 1. Experimental Scheme of the ZnO nanowire growth, electroless deposition, and characterization of the NWs/Ag shealth composites.

2.2 EL and EB silver deposition on ZnO NWs and on a silicon surface

The concentrated solutions for the silver plating were received from Peacoak Lab and further diluted with de-ionized water. The dilution factors were 1:100 ratio by volume for silver solution “A” (25%-30% wt silver diammine and 10-15% wt ammonium hydroxide in

water), activator solution "B" (sodium hydroxide 10%wt and ammonium hydroxide 5%wt in water), reducer solution "C" (1%wt Formaldehyde in water) and sensitizer solution (20%wt propyl alcohol, 5%wt hydrochloric acid and 5%wt stannous chloride in water). Scheme 1b and c illustrate the sensitization and silver plating process [16]. Firstly, the substrate with the NWs was immersed into the diluted stannous chloride solution, and then extra Sn^{2+} ions were removed by de-ionized water rinsing and keeping the surface wet. Hence Sn^{2+} ions were absorbed on the surface of the ZnO NWs via electrostatic interaction. Secondly the mixture of equal amounts of diluted silver, activator, and reducer solutions was poured onto the substrate and kept there. During this process, the surface Sn^{2+} ions were oxidized to Sn^{4+}, while the Ag^{+} ions were reduced to neutral Ag and deposited on the ZnO nanowire surface uniformly. Finally, the surface was rinsed with DI-water and dried under flowing nitrogen. Experimentally, 10 to 20 seconds of reaction time would usually give a homogeneous coverage with a high density of silver 3D islands on the NW surface.

For comparison, a bare silicon substrate was covered with 6 nm of silver using an FC-2000 Temescal E-Beam Metals Evaporation system, at an evaporation rate of 1 Å/s.

2.3 SEM and SERS investigations of silver coated silicon and NWs surface

The topography and chemical composition of EB and EL deposited silver nano structures deposited on the ZnO NWs and on the silicon surfaces were investigated using a LEO SUPRA 55 scanning electron microscope (SEM) with energy dispersive x-ray (EDX) capabilities. The dielectric ZnO NW core/Ag sheath composites as prepared above were then immersed in a solution of benzenthiol ($10^{-4}M$) for 6 h, and dried for SERS studies to investigate the silver stabilization properties with laser scanning and exposure time in the air. The SERS measurements were carried out utilizing a confocal μ-Raman system which consisted of a Mitutoyo Microscope and an Ocean Optics QE65000 spectrometer equipped with a thermoelectrically cooled CCD. The 514.5 nm line of an Ar ion laser was used as the excitation source. The microscope utilized a 100X 0.7 NA objective for focusing the laser light and was coupled to the spectrometer through a fiber optic cable.

3. RESULTS AND DISCUSSION

3.1 SEM characterization of ZnO NWs as grown

Representative SEM images of the ZnO NWs as grown on Si (100) are shown in Figure 1 and Figure 2.

ZnO NWs can be grown with or without a gold catalyst and in our experiment, we employed bare silicon substrate without any metal catalyst. It is clear that the tip is free of a metal cap, confirming the catalyst free growth process via the vapor-solid (VS) growth mechanism [15]. As shown in Figure 1, different density, geometry, length and diameter of the NWs can be obtained by controlling the growth conditions, such as the furnace tube size, gas flow rate, growth time, and the distance between the substrate and the source material.

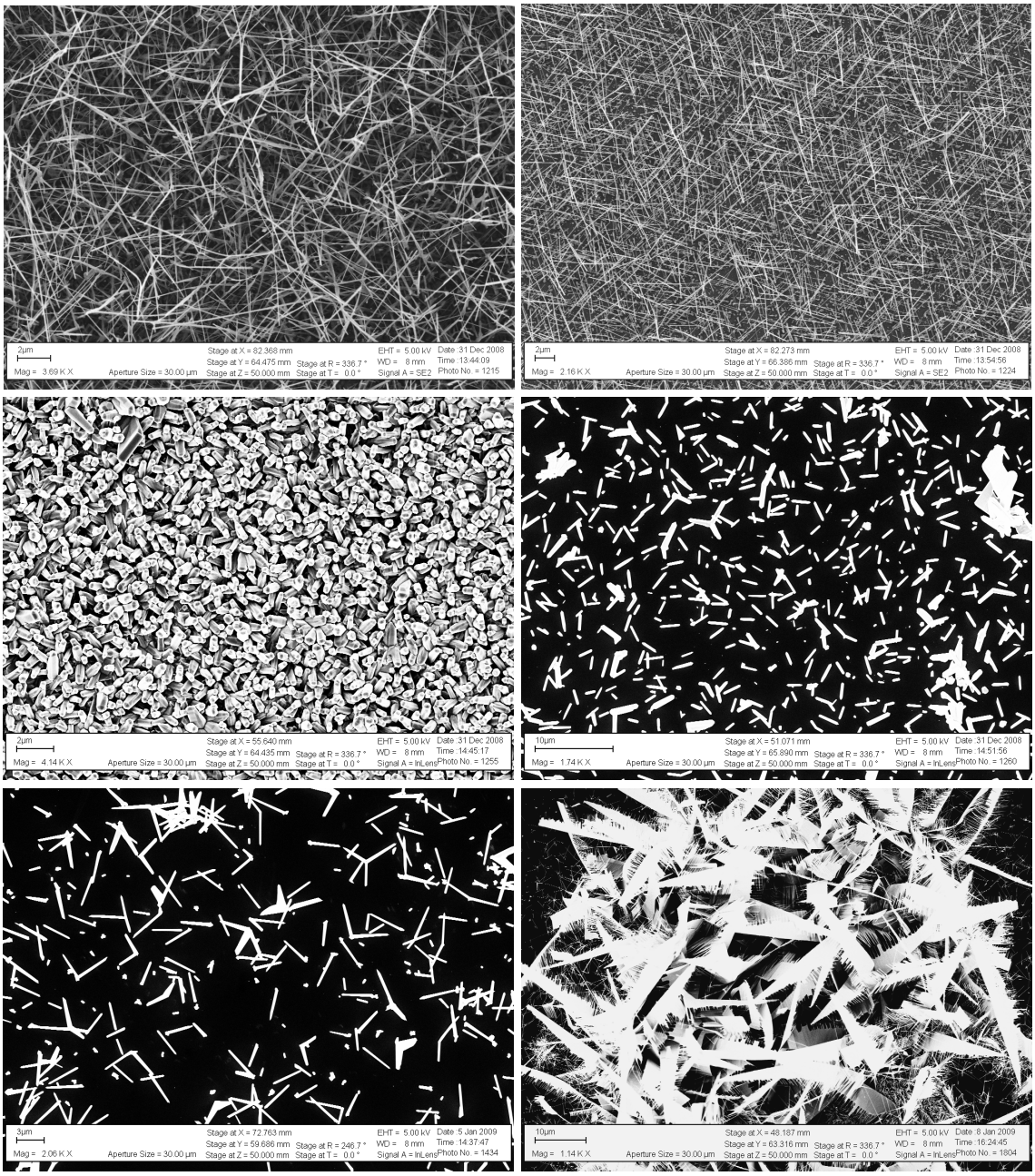

Figure 1 SEM images of ZnO growth. Representative SEM images of ZnO nanowires grown on Si with different geometries;

Figure 2 shows high resolution SEM images of the individual nanostructures as grown. Different NW shapes, including single, angled crossing, "Y" shapes, "star" shapes and "nano-saw" shapes formed. The diameters varied from 50 nm to 300 nm, and the length was on the

order of several microns. Energy dispersive x-ray (EDX) analysis indicated that the chemical composition of the NWs was stoichiometric ZnO.

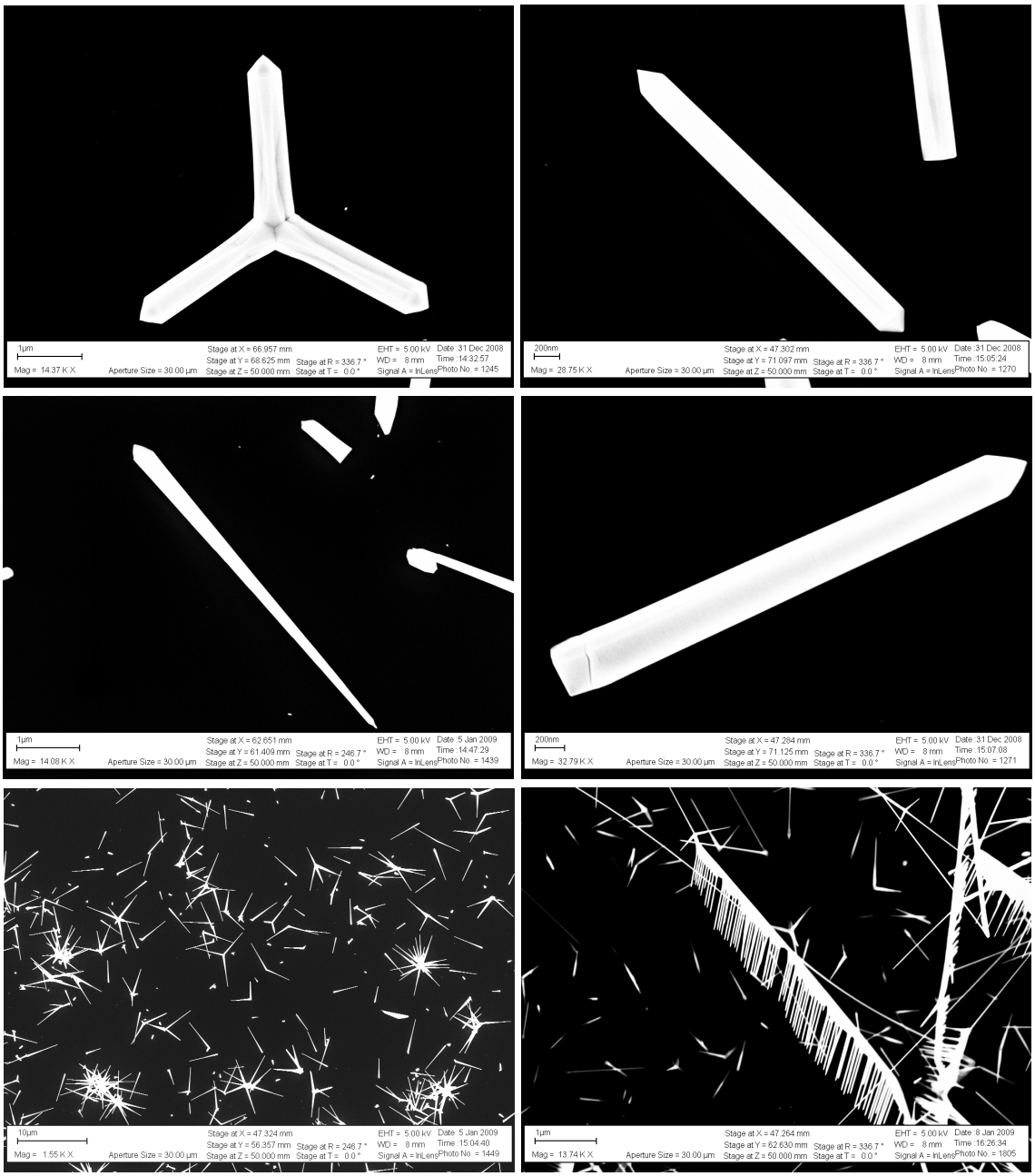

Figure 2 Representative SEM images of ZnO nanowires grown on Si with different geometries;

3.2 SEM characterization of silver coated NWs

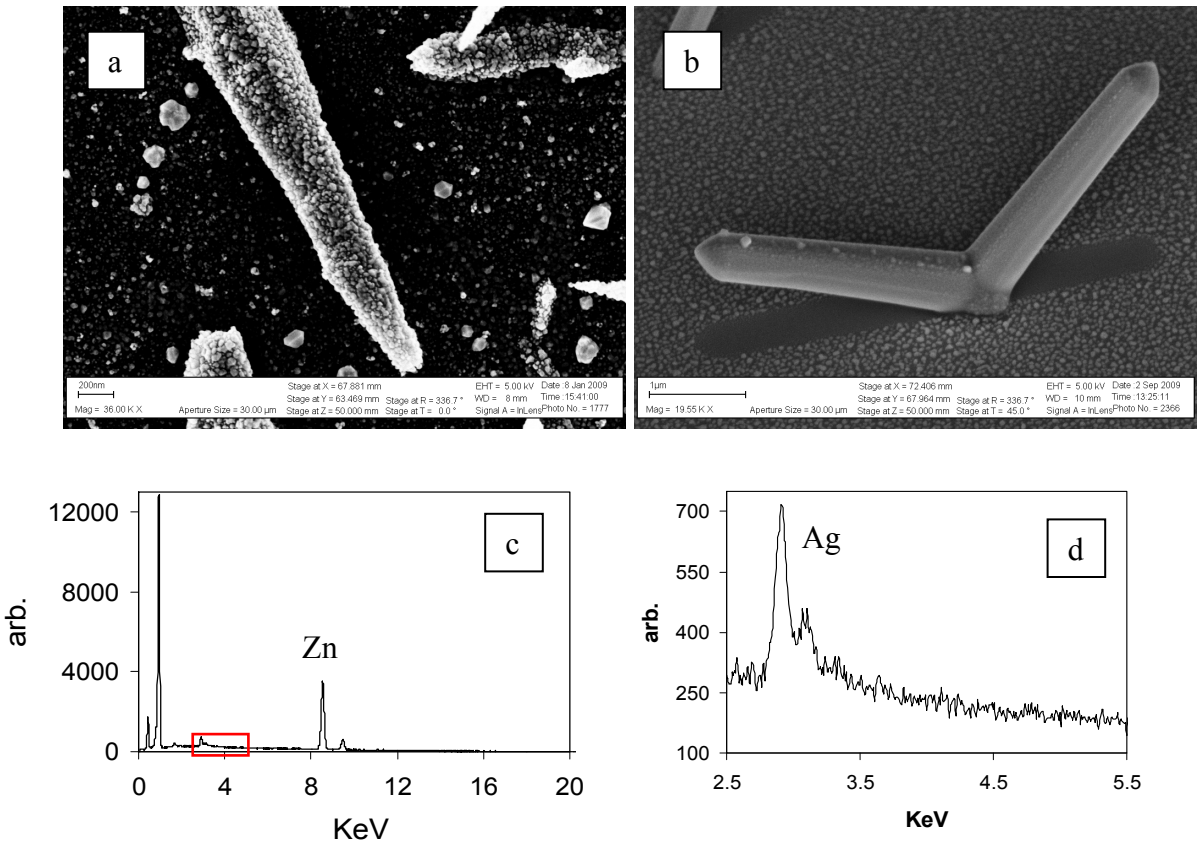

Figure 3 SEM images of EL (a) and EB (b) silver coated ZnO NWs, and energy diffraction x-ray (EDX) analysis of EL coated NWs.

Figure 3a shows the tip of an electroless silver coated ZnO NW, which displays 3D islands with diameters on the order of 20nm. In addition electroless silver islands were distributed more uniformly on the NWs than those on bare silicon, which indicates the morphology of silver not only depends on the deposition approach, but also is related to the substrate or substrate geometry. The most likely explanation for these results is that the surface structure, faceting and curvature or surface energy affects the nucleation of the metal islands. As can be seen in Fig. 1a, the advantages of EL silver plating overcomes the shortcomings of the EB evaporation technique, which cannot deposit the metal around the whole NW, since it is a line-of- sight process. This also becomes a problem for closely aligned vertical NWs or other oriented structures, as shown in Figure 3b, in which e-beam evaporation was used. Also note the high metal island coverage on the Si substrate in Fig. 1b, which is not the case in the EL process (Fig. 1a), supporting the idea that the geometry and surface morphology is also important in the case of nucleation in the EL process. In addition, EL plating is a very inexpensive technique with potentially large throughput, which is not possible in the EB deposition case.

Figures 3c and 3d show the EDX results for the EL Ag covered ZnO NWs shown in fig. 1a, and a close-up of the curve of the silver EDX peak region. The peaks at 1.03 KeV, 8.62 KeV and 9.59 KeV can be assigned to Zn [17, 18], and the weak features at 2.98 KeV and 3.14 KeV are attributed to Ag [19, 20]. This result confirms the depositions of silver particles on the NWs.

3.3 Ag stability investigation via SERS

The SERS investigations were performed with a laser power of 0.75 mW and a laser diameter of 600 nm on the sample. A large number of SERS measurements were performed on the newly prepared samples in order to investigate the time dependence behavior. As shown in Figure 4a, the main line of BZT at 1576 cm^{-1} remained steady on the electroless silver covered NWs, indicating good stability of the freshly prepared silver sheath NWs under relatively short laser irradiation, and the power of 0.75 mW did not result in damage to the benzenethiol or the EL coated Ag layer.

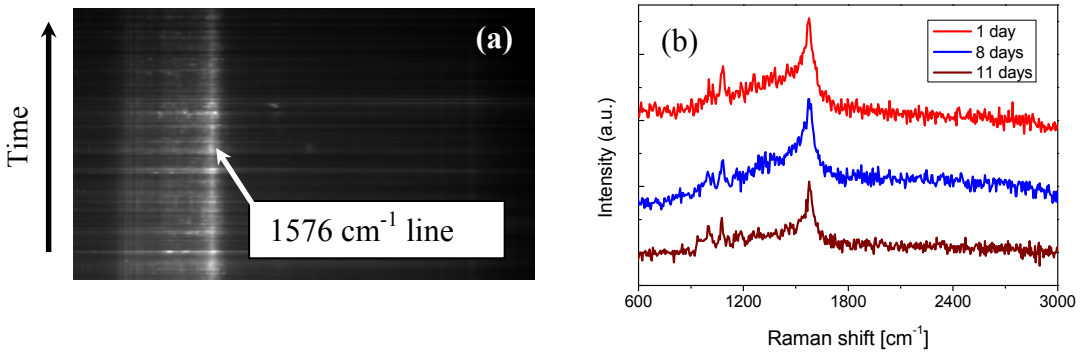

Figure 4. *(a) Time dependent behavior of Ag on NW produced by electroless (EL) depositions. (b) Surface enhanced Raman spectroscopy (SERS) on ZnO NW core/Ag shealth composites with the process of time in air.*

To examine the stability to oxidation of the silver nanoparticles, SERS measurements were carried out on the same single dielectric ZnO nanowire core/silver sheath composite produced by EL plating, and benzenethiol (BZT) served as the SERS-active molecule. A single NW was randomly selected for SERS measurements and monitored for the signal strength from the moment that the composites were fabricated. Figure 4(b) shows representative spectra which were obtained on the EL generated nanowire/silver structures after the samples were exposed in air for several days. The major Raman peaks at 1002, 1071, and 1576 cm^{-1} can be assigned to symmetric ring breathing modes, in plane C-H bending modes, and in plane C-C stretching modes of the phenyl ring of benzenthiol [21-26], respectively. In comparison with the spectrum obtained on the first day, the intensity of the main SERS signal at 1576 cm^{-1} does not show a significant decrease as a function of time in

the atmosphere, which suggests that the thiol attachment to the Ag surface protects the silver from oxidation for this time period.

However, once these structures were left in the atmosphere for longer times after fabrication, SERS mapping of these structures suggested that the composites did gradually degenerate. Figure 5(a) shows the SERS mapping results of the dielectric ZnO nanowire core/silver sheath composite at 1576 cm^{-1}, and its corresponding microscope images including before and after laser scanning (Figure 5(b) and 5(c)). This sample was produced by the EL plating process, and the sample was kept in the air for eight days. The mapped region was a 4×4 micron square. As shown in the map, strong SERS signal was obtained on the nanowire core/silver sheath composite region, while no SERS signal was observed on the bare silicon wafer (blue regions). However, exposure to the laser beam led to the near disappearance of the NW in the optical microscope (Figure 5(b) and 5(c)), which may be attributed to the deterioration of the Ag coating, leading to a loss of contrast and visibility in the optical microscope. In fact, the NWs are just barely visible if viewed through the microscope eyepiece. When this sample was examined with AFM/TERS after the mapping was finished, a complete loss of detectable SERS signal was noted. This observation indicates that although initially, the Ag is protected by the thiol layer, gradual oxidation in air does occur.

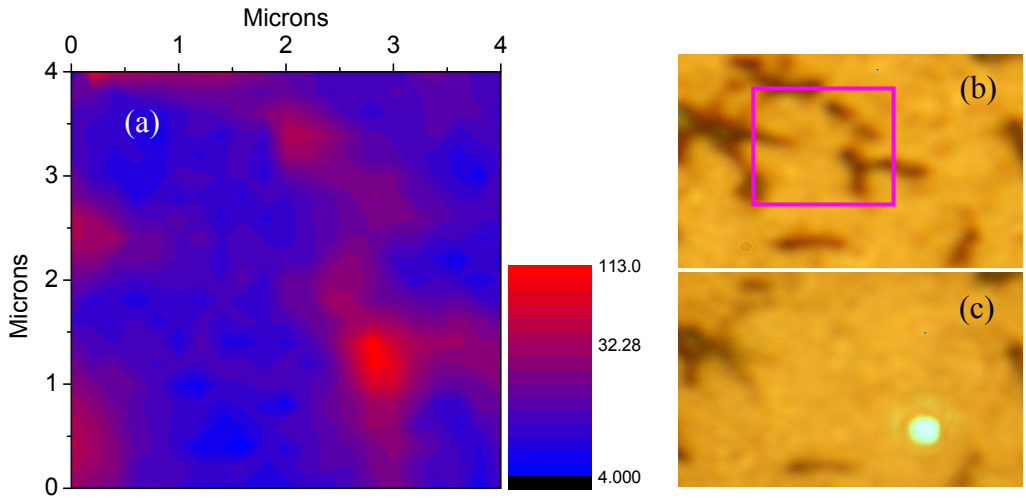

Figure 5 *(a) Surface enhanced Raman spectroscopy (SERS) mapping of ZnO NWs core/silver sheath composites at the line of 1576 cm^{-1}; (b) and (c) microscope images before and after performing the mapping.*

3.4 Ag NPs stabilization investigation via EDX

It is well known that properties, such as the melting temperature, depend on size, shape and dimensionality of the nano structures. The small size usually means a large surface to volume ratio and a higher surface energy than the bulk, as well as a larger surface energy. Here we demonstrate that the silver oxidation process also depends on the size of the nanostructures. In order to investigate the stability of a silver layer with a broad particle size

distribution, Ag NPs were deposited on bare silicon via the EL chemistry process. This flat substrate exhibited a much broader size distribution in the range of 5-100 nm than on the curved NWs, as shown in Figure 6(a). A piece of the flat silicon covered with the EL plated silver NPs was stored in air after the silver plating. Energy diffraction X-ray (EDX) was performed in order to obtain the silver oxidation rate. Although the oxidation rate is irregular, as shown in Figure 6(b), it is obvious that the oxygen amount in Ag NPs is increasing with the process of time.

To further examine the dependence of the oxidation process on the silver NP size distribution, a layer of 6 nm of silver was deposited on a bare silicon piece by E-beam evaporation, at an evaporation rate of 1 Å s^{-1}. As shown in Figure 6(c), the EB evaporated silver particle size was in the range of 15-55 nm with a mean diameter of 35 nm. As can be seen, the oxidation rate of the EB produced silver is slower than that formed by the EL chemical plating approach (Figure 6d). These results suggest that the particle size, as well as the particle size distribution, can have a significant effect on the oxidation rate.

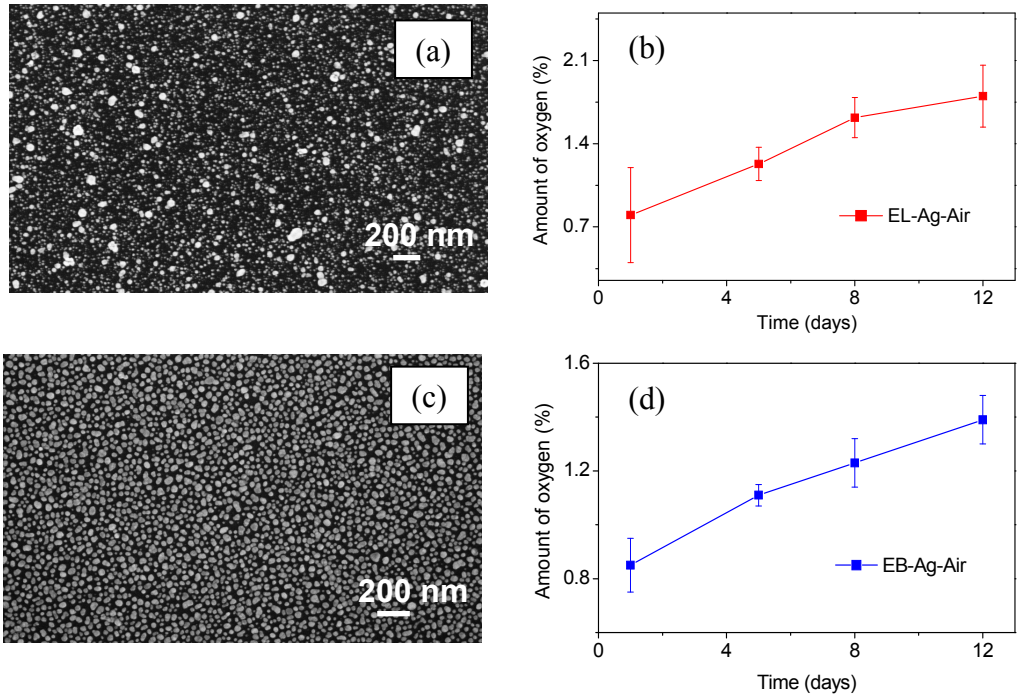

Figure 6. *SEM images of silver NPs on silicon surface produced by EL plating (a) and EB coating(c); (b) and (d) plot of oxygen amount vs time.*

4. SUMMARY

The stability of silver nano structures has been studied by investigating the change of the amount of oxygen as a function of time in the atmosphere, using the Si/Ag system, produced via electroless (EL) plating and e-beam (EB) deposition. SERS measurements on NW/Ag NPs

composites were also performed, indicating that a monolayer of benzene thiol can protect the silver surface for more than ten days. Our results also demonstrate that the sharp distribution of very small Ag NPs produced by EL show significantly enhanced oxidation rates compared to those formed by EB approach. These results provide useful information on the silver nano structure oxidation process which should be helpful in extending the silver lifetime for various applications.

5. ACKOWNLEGEMENT

This work was supported by the Office of Naval Research (ONR) and Nanoscience Institute (NSI) of the US Naval Research Laboratory.

6. REFERENCES

[1] K. M. Manesh; A. I. Gopalan; K. P. Lee and S. Komathi Catal. Commun. 11, 913-918, (2010).
[2] Wang, G. F.; Stender, A. S.; Sun, W.; Fang, N.; Analyst 135, 215-221, (2010).
[3] Wong, V.; Ratner, M. A. J. Phys. Chem. B 110, 19243-19253, (2006).
[4] Akimov, Y. A.; Koh, W. S. Nanotechnology 21, 235201 (2010).
[5] Nelayah, J.; Kociak, M.; Stephan, O.; de Abajo F. J. G.; Tence, M.; Henrard, L.; Taverna, D.; Pastoriza-Santos, I.; Liz-Marzan, L. M.; Colliex, C.; Nat. Phys. 3, 348-353, (2007).
[6] Arnim, H. *Chem. Mater.*, 10, 444–450, (1998).
[7] Reetz, M. T.; Helbig, W.; *J. Am. Chem. Soc.*, 116, 7401–7402, (1994).
[8] N. Leopold; and B. Lendl *J. Phys. Chem. B*, 107, 5723–5727, (2003).
[9] W. Tu and H. Liu *Chem. Mater.*, 564–567, 12, (2000).
[10] Y. Nagata; Y. Watananabe; S. Fujita; T. Dohmaru; and S. Taniguchi; *J. Chem. Soc., Chem. Commun.*, 114, 1620-1622, 1992,
[11] W. Wu; Y. Wang; L. Shi; Q. Zhu; W. Pang; G. Xu; and F. Lu *Nanotechnology* 16, 3017, (2005)
[12] A. L. Stepanov; D. E. Hole and P. D. Townsend J. Non-Cryst. Solids 260, 65-74, (1999).
[13] C. Balasubramanian; V. P. Godbole; V. K. Rohatgi; A. K. Das and S. V. Bhoraskar *Nanotechnology* 15, 370, (2004).
[14] K. A. Bogle; S. D. Dhole and V. N. Bhoraskar, Nanotechnology 17, 3204-3208 (2006).
[15] Prokes S. M.; Glembocki, O. J., Rendell, R. W. and Ancona, M. G. *Appl. Phys. Lett.* 90, 093105, (2007).
[16] Qi, H.; Alexson, D.; Glembocki, O.; and Prokes, S. M. *Nanotechnology 21*, 085705, (2010).
[17] Liu, S.; Zhang, H. and Swihart, M. T. *Nanotechnology* **20,** 235603, (2009).
[18] Büsgen, T.; Hilgendorff, M.; Irsen, S.; Wilhelm, F.; Rogalev, A.; Goll, D.; and Giersig, M. *J. Phys. Chem. C 112,* 2412, (2008).
[19] Gao, Y.; Shan, D.; Cao, F.; Gong, J.; Li, X.;, Ma, H.; Su, Z. and Qu, L. *J. Phys. Chem. C 113,* 15175, (2009).

[20] Chuang, H. Y. and Chen, D. H. *Nanotechnology* **20,** 105704, (2009).
[21] Jiang, C.; Lio, W.; Tsukruk, V. *Phys. Rev. Lett.* 95, 115503, (2005).
[22] Ding, J.; Birss, V.; Liu, G. *Macromolecules* 30, 1442, (1997).
[23] Sears, W.; Hunt, J.; Stevens, J. *J. Chem. Phys.* 75, 1589, (1981).
[24] Zucolotto, V.; Ferreira, M.; Cordeiro, M.; Constantino, C.; Balogh, D.; Zanatta, A.; Moreira, W.; Oliveira, O. *J. Phys. Chem. B* 107, 3733, (2003).
[25] Aroca, R.; Thedchanamoorthy, A.; *Chem. Mater.* 7, 69, (1995).
[26] Kim, J. H.; Kang, T.; Yoo, S. M.; Lee, S. Y.; Kim, B.; Choi, Y. K. *Nanotechnology* **20,** 235302, (2009).